Case Studies in Chemical and Environmental Engineering 8 (2023) 100492

Contents lists available at ScienceDirect

Case Studies in Chemical and Environmental Engineering

journal homepage: www.sciencedirect.com/journal/case-studies-in-chemical-and-environmental-engineering

Case Report

Variability in odour impact assessment due to different cloud cover estimation approaches: A northern Italy case study

Francesca Tagliaferri, Laura Facagni, Marzio Invernizzi *, Selena Sironi

Politecnico di Milano, Department of Chemistry, Materials and Chemical Engineering "Giulio Natta", P.za Leonardo da Vinci 32, 20133, Milano, Italy

A R T I C L E I N F O

Keywords:
Cloud cover (CC)
Dispersion modelling
CALPUFF model
Odour impact assessment
Intercomparison

A B S T R A C T

For atmospheric dispersion models, Cloud Cover (CC) is an input that controls turbulent diffusion. This study analyses the influence of various approaches to estimate CC in odour dispersion modelling: given the normative relevance of these assessments, it is pivotal to understand the result of different operational choices about this parameter. Results seem largely comparable regardless the different CC approach. Both, micrometeorological parameters from CALMET simulations and CALPUFF odour impact maps appear almost overlapped. The outcome of the present study is that CC algorithms, do not significantly influence odour impact: this result strengthens the regulatory use of models for odour assessments.

1. Introduction

As a result of rapid population and industrial growth in recent decades, the amount of pollutants discharged into the environment is continuously rising [1,2].

Concerning air quality, people frequently contact municipal authorities to complain about nuisances generated by odourous emissions, which are typically associated to industrial and agricultural facilities [3,4].

Nowadays, odours are monitored and regulated in many countries [5]. Therefore, the development of various strategies able to estimate or predict chemical exposure [6,7], particularly odour, on citizens represents a relevant issue [8,9]. Dispersion models are algorithms that can simulate the spatial-temporal concentration field of the pollutant species released by emission sources, hence estimating areas of population exposure as well as ground level contamination concentrations [10–12].

CALMET/CALPUFF is a sophisticated modelling system, frequently adopted for odour impact assessment studies. It generates three-dimensional gridded meteorological data (such as hourly wind and temperature fields) in the computational domain via refined treatment and assimilation of available surface and upper air observations and geophysical data [4,13,14].

Concerning CALMET meteorological processor, Cloud Cover (CC) represents a crucial input variable since its definition might involve a significant degree of uncertainty. According to Stull (2016) [15], the fraction of the sky covered by clouds is commonly referred to as "sky cover" or "cloud cover".

Clouds originate throughout all the levels of the atmosphere and affect both weather and climate [15,16]. The type and the amount of clouds that commonly form over a region impact the precipitation conditions, and it also influences air temperature at the ground [17,18]. It is estimated in terms of how many eighths of the sky are covered by clouds, ranging from 0 oktas (completely clear sky) to 8 oktas (completely overcast) according to the World Meteorological Organization [16].

CC can be estimated in different ways, either through direct observation of the sky or through theoretical methods from other known meteorological parameters [18,19].

However, until now, due to a limited worldwide network of observation stations, which is often non-existent in many regions, large uncertainties in CC measurement still remain [19]. Moreover, the evaluation could be difficult if some of the clouds are only partly visible or temporarily completely concealed [18]. As a result, theoretical approaches have been also proposed to estimate numerically CC data.

For this reason, the present study analyses the influence on the results of CALPUFF odour dispersion modelling of four different approaches to estimate CC parameter, discussed in Section 2.3.

The simulation domain is located in the south of Milan, in Lombardy Region (Italy). This region is noted for having the largest number of residents in Italy as well as high levels of industrialisation.

The Po Valley's topographical features significantly influence the local meteorology, leading to the typical climate of the region

* Corresponding author.
E-mail address: marzio.invernizzi@polimi.it (M. Invernizzi).

https://doi.org/10.1016/j.cscee.2023.100492
Received 17 July 2023; Received in revised form 11 September 2023; Accepted 12 September 2023
Available online 16 September 2023

characterized by low winds, particularly weak in the winter months. Therefore, air pollution remains a severe problem in Lombardy region.

Odour impact is estimated by running CALMET simulations with input met dataset that differ solely in terms of CC.

Results are elaborated in accordance with the Regional Guide of Lombardy [20]: impact maps must be referred to the peak odour concentration values, expressed in terms of 98th percentile on an annual basis.

Although this guideline emphasizes that there is no unanimous agreement on the definition of a peak-to-mean factor in the scientific literature, a constant value of 2.3 is proposed [20] and adopted in the present study for post-processing the simulation results.

In conclusion, considering the difficulty involved in CC estimation, the aim of this research is to evaluate how the selection of several methods for quantifying CC data affects the results of odour dispersion modelling.

2. Methods and materials

2.1. CALPUFF

CALPUFF is an advanced, integrated Lagrangian puff modelling system for the simulation of atmospheric pollution dispersion. It includes three main components: 3D meteorological model CALMET, air quality dispersion model CALPUFF and the postprocessing tool CALPOST.

CALPUFF is a non-steady-state Lagrangian Gaussian puff model that simulates individual puffs of pollutant emitted into the atmosphere and spread outward from the centre of the plume in both a horizontal and vertical direction. More specifically, the plume is dispersed into the atmosphere according to a normal statistical distribution and in response to time and space-varying local conditions. CALPUFF is able to simulate pollutants emission from point, area, volume and line sources.

In particular, it includes specific algorithms for complex terrain, building downwash effect, overwater transport, transitional buoyant and momentum plume rise, rain cap effects, coastal interaction effects, wet and dry removal, and simple chemical transformations. For these reasons, CALPUFF represents an adequate model for near-field transport (i.e., <50 km). Indeed, US-EPA [21] recommends CALPUFF as an alternative model for near-field transport (i.e. < 50 km). The EPA recognizes that, in case of complex terrain and complex winds, AERMOD preferred model, as a Gaussian plume model, may be not appropriate to address such situations. Conversely, CALPUFF or other Lagrangian models may be more suitable. Therefore, considering the typical meteorological conditions of the simulation domain, characterized by a high frequency of wind calms at ground level, CALPUFF can be considered an appropriate simulation tool.

The model adopted is consistent with the Lombardy Region Guideline [20] and the Italian National Guideline [22], which encourage using Lagrangian (puff or particles) models for regulatory purposes.

CALPUFF output files contain either hourly concentrations or hourly deposition fluxes evaluated at selected receptors. CALPOST is used to process these files and generate statistics, such as the maximum or the nth percentile of the hourly-average concentrations at each receptor.

The files associated with the modelling system, e.g., executables/source code, preprocessors, associated utilities, and documentation can be found on Exponent's website (http://www.src.com/calpuff/download/download.htm).

2.2. CALMET

CALPUFF modelling system is coupled with CALMET meteorological pre-processor, which provides diagnostic 3D wind and temperature fields for CALPUFF dispersion simulation, starting from meteorological measurements, orography and land use data [23].

The diagnostic meteorological model CALMET includes specific algorithms for calculating micro-meteorological variables of the planetary boundary layer on both land and water [23].

Using these algorithms, CALMET is able to reconstruct, besides wind and temperature fields over a simple or a complex orographic domain, two dimensional fields of micrometeorological variables such as mixing height or Monin Obukhov length [24].

CALMET includes a diagnostic wind field generator able to account for kinematic effects of the terrain, slope flows and blocking effect on the wind flow.

It is recognized as a suitable tool to generate input met data for atmospheric dispersion models, which demand micrometeorological data and the mean wind field for an accurate representation of atmospheric turbulence.

To run CALMET simulations, it is necessary to provide meteorological input data, as discussed in Paragraph 2.2.1, as well as to define some CALMET-specific parameters (Paragraph 2.2.2), that are required to compute 3D wind fields.

2.2.1. Meteorological data

Meteorological data collection and pre-processing represents a crucial step in atmospheric dispersion modelling [25]. The amount and the quality of input data requirements, such as wind speed [m/s], wind direction [°], relative humidity [%], temperature [°C], CC [tenths], and solar radiation [Wh/m^2], depend on the complexity of the model. Sophisticated, non-steady-state models, as CALPUFF/CALMET modelling system, can process a 3D dataset of met data.

In principle, met data could be measured from meteorological stations or simulated from prognostic models. In this work, observed surface and upper air station data (for the reference year 2016) are implemented for all the simulations. The investigated CC parameter, as discussed in section 2.3, is obtained from measured data or theoretical approaches.

The hourly surface meteorological observations (i.e. wind direction, wind speed, temperature, relative humidity, atmospheric pressure and solar radiation) were provided by the Regional Agency for Environmental Protection (ARPA Lombardia, Milan, Italy) for the station of Landriano Cascina Marianna LDR (45.32°N, 9.27°E) inside the computational domain, 2 km away from the simulated odour source.

The upper air data were acquired from NOAA/ESRL Radiosonde Database (https://ruc.noaa.gov/raobs/), in particular from Milano Linate International Airport LIML (45.43°N, 9.28°E), 13 km away from the source.

To treat possible invalid or missing data obtained from measurement stations, the US-EPA protocol [21] and the Lombardy Region Guideline [20] were adopted as reference.

For use in regulatory dispersion modelling, the US-EPA reference demands a percentage of missing data of less than 10% over the entire meteorological dataset. The same document recommends various substitution procedures (e.g. persistence, interpolation, profiling) depending on the nature of the application, the availability of alternative sources of meteorological data, and the extent of the missing or invalid data.

According to Lombardy Guideline, the percentage of missing data for each met variable, must be less than 20% over the entire dataset and less than 70% for each month.

The meteorological dataset adopted for the present case-study complies with the abovementioned criteria about missing data. Interpolation procedure is adopted to replace missing data.

2.2.2. CALMET parameters

To run simulations, CALMET requires necessarily the definition of some parameters [14,24,26]. If available, US-EPA recommended values [27] or CALMET default values were generally adopted. Instead, for TERRAD, BIAS, R1, R2 RMAX1, RMAX2 and MCLOUD parameters no default values or clear suggestions in the Model User's Guide are available.

Table 1 lists the numerical values, for the abovementioned parameters, adopted to run the simulations. The choice of these values will be briefly discussed.

TERRAD parameter defines the radius of influence of terrain features. This variable is necessary to execute CALMET simulations for all the investigated input meteorological settings [28]. A sensitivity study was conducted to find out the optimal TERRAD to minimize the Root Mean Square Error (RMSE) of the wind speed by comparing the CALMET output values with the observed measurements. Due to the flat orography, the resulting RMSE for each value of TERRAD were almost identical, with slight differences examining the fifth decimal number. Therefore, a TERRAD value of 3 km was adopted by choosing the RMSE with the lowest fourth decimal number.

The weight of surface wind observations to interpolate winds at higher levels in the computation of the initial guess field [28] is controlled mostly by the BIAS parameter, required for “OBS” and “HYBRID” simulations.

Negative BIAS reduces the weight of upper air stations (e.g. −1 means that upper-air observations are not taken into account in the interpolations for this layer), positive reduces the weight of surface stations.

In the first layer, surface observations were given 100% of the weight (BIAS = −1) and zero weight (BIAS = 1) in the final two vertical levels. According to Rzeszutek (2019) [24]and Rood (2014) [25], a gradation of weights was attributed to the intermediate layers, with the fourth layer receiving equal weight (BIAS = 0).

To run “OBS” and “HYBRID” simulations, the definition of R1, R2, RMAX1 and RMAX2 is mandatory. R1 and R2 represent the weight of each station inside the domain in the computation of the wind field [28]. Due to the presence of a single station, one for the surface and one for the upper air data, these parameters were set as to cover the entire domain [29].

Therefore, R1, which refers to the surface layer, was identified as the greatest distance from the station to the domain’s farthest point, i.e. 5.7 km. Given that the upper air station is outside the simulation domain, R2, referred to layers aloft, was determined to be the domain diagonal, i. e. 8.5 km.

RMAX1 and RMAX2 parameters refer to the maximum radius of influence for surface and upper data, respectively, over land surfaces. These parameters were set equal to twice R1 and R2 [28,30], as recommended by the scientific literature.

Finally, to investigate the influence of CC, MCLOUD parameter, which identifies the available options to compute cloud fields [28], is set equal to 1. This way CALMET processes the user-provided CC parameters as input in the implementation of the surface observational data.

2.3. Cloud cover parameter

CC can be estimated in different ways, either through direct observation of the sky or through theoretical methods from other known meteorological parameters [19].

This work investigates the following approaches to estimate CC parameter, and their influence on the simulated odour impact maps.

Table 1
Selection of parameters for CALMET setup.

Parameters		
TERRAD	3	[km]
R1	5.7	[km]
R2	8.5	[km]
RMAX1	11.4	[km]
RMAX2	17	[km]
MCLOUD	1	/
BIAS	−1, −0.67, −0.33, 0, 0.2, 0.4, 0.6, 0.8, 1, 1	

2.3.1. Approach 1: METAR

The World Meteorological Organization (WMO) describes METAR as the aerodrome routine meteorological report, or as aviation weather report [16].

METARs typically come from airports or permanent weather observation stations, generating data once an hour or half-hour at most stations. A typical METAR contains information about temperature, dew point, wind direction and speed, precipitation, CC, visibility and barometric pressure.

2.3.2. Approach 2: ERA5

ERA5 is the fifth generation of reanalysis data, available from 1940 onwards, elaborated by the European Centre for Medium-Range Weather Forecasts (ECMWF) [31].

Reanalysis combines model data with observations from around the world to generate a complete and consistent dataset using the laws of physics. This data assimilation is based on the approach taken by numerical weather prediction centers, which integrates a previous forecast with newly available observations in an optimal way to provide a new best estimate of the condition of the atmosphere.

ERA5 offers a large number of atmospheric, ocean-wave and land-surface quantities, including CC parameter, on an hourly basis.

The data set was obtained by means of the website https://cds.climate.copernicus.eu.

2.3.3. Approach 3: relative humidity

CC fraction can be estimated through theoretical correlations by knowing the relative humidity, since it has been demonstrated [32–34] a direct proportionality between these two meteorological parameters.

Heat is transferred to the air from the surface, resulting in hydrostatic instability. The air will then rise due to a vertical pressure gradient, and as the air cools with height, the relative humidity will increase, assuming all other humidity parameters constant. Then, the air becomes saturated and clouds form when the relative humidity hits 100%.

The empirical relation between the total CC fraction and the relative humidity (RH) at the surface is reported in the following equation (eq. (1)):

$$CC = k(RH - RH_0) \tag{1}$$

Where $k = 1.28$ and $RH_0 = 0.34$ [32–34]

2.3.4. Approach 4: solar radiation

According to scientific literature [35–39], clouds are the primary modulators of the shortwave and longwave radiation components of the Earth’s energy balance and, as such, contribute to regulate the temperature of the planet.

Incoming solar radiation (K) is monitored by various meteorological sites. If such measurements are available, these can be used directly to evaluate the total CC by the calculation of the solar elevation angle (φ) [17,35,36]. After estimating the solar elevation angle, it is necessary to quantify the clear sky solar radiation (K_0) (eq. (2)):

$$K_0 = a_1 \sin \varphi + a_2 \tag{2}$$

with $a_1 = 910$ and $a_2 = -30$ [37,38]

Then, from the solar radiation measured by the surface station ($\boldsymbol{K}$), the CC can be estimated (eq. (3)):

$$K = K_0\left(1 + b_1 * CC^{b_2}\right) \tag{3}$$

with $b_1 = -0.75$ and $b_2 = 3.4$ [37,38].

According to Holtslag and Van Ulden (1983) [37], the constants a_1, a_2, b_1, and b_2 are specifically referred to the geographical location where the CC is to be estimated. The above-mentioned constants, adopted in the present study, are referred to Hamburg (Germany), as the closest place to the simulation domain in terms of latitude and longitude within the available dataset.

To resume, as previously discussed, the measuring network of ARPA Lombardia does not offer CC data, which is therefore estimated (for the reference year, 2016, on an hourly basis) according to different approaches.

- "METAR": meteorological database of the Iowa State University, for the station of Milano Linate International Airport LIML (45.43°N, 9.28°E), 13 km away from the source.
- "ERA5": reanalysis database of the European Centre for Medium-Range Weather Forecasts, for the station of Milano Linate International Airport LIML (45.43°N, 9.28°E), 13 km away from the source.
- "Relative Humidity": empirical relationship in which relative humidity (RH) values are measured from the surface station of Landriano Cascina Marianna LDR (45.32°N, 9.27°E), located inside the domain, 2 km from the source.
- "Solar Radiation": empirical relationship in which solar radiation (K) values are measured from the surface station of Landriano Cascina Marianna LDR (45.32°N, 9.27°E), located inside the domain, 2 km from the source.

2.4. Site domain

For the simulations, a square domain of 6 km × 6 km, with a mesh grid of 100 m, was identified. Ten vertical layers are identified with the cell face heights at 10, 30, 60, 120, 240, 480, 920, 1600, 2500, and 3500 m; giving a total of 36,000 cells in the domain.

The computational domain (white square in Fig. 1, right) is located in the south of Milan, Italy (SW corner: 45.29°N, 9.21°E), with a flat orography, as shown in Fig. 1, left.

To elaborate the simulation results, odour concentration is computed on a set of selected discrete receptors located inside the computational domain. To this purpose, a receptor nest was created by locating 324 receptors, radially separated by an angle of 20°, at distances of 50, 100, 150, 200, 400, 600, 800, 1000, 1200, 1400, 1600, 1800, 2000, 2200, 2400, 2600, 2800 and 3000 m from the source centre, according to the scheme shown in Fig. 2.

2.5. Emission source

The emission source, identical for each simulation, is an industrial stack located in the centre of the domain. CALPUFF model involves the definition of some specific dimensional parameters for point sources: the diameter and the height of the stack, the temperature and the velocity of the exit air flow.

Concerning the emissive data, it is necessary to quantify the pollutant emission rate. In case of odour emissions, the key parameter is represented by the amount of odour emitted per unit time (Odour Emission Rate, OER).

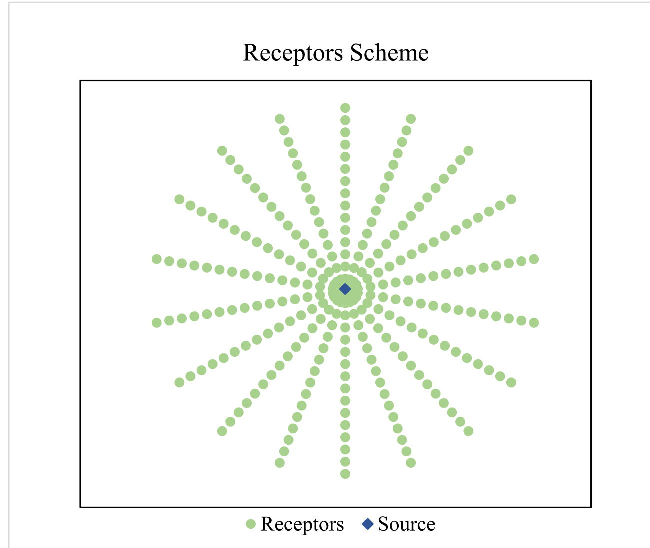

Fig. 2. Receptors scheme forming a nest.

The parameters referred to the point source are resumed in Table 2; no temporal variability of the emission is considered.

Finally, to set the simulations, MDISP parameter is defined. It identifies the approach adopted to compute horizontal and vertical dispersion coefficients. In the present study, MDISP is set equal to 2, as suggested by US EPA [24,27]. It means that the computation of turbulence-based dispersion coefficients is derived from micrometeorological variables.

3. Results and critical discussion

3.1. CALMET meteorological pre-processor output

It is worth to examine CALMET output, in terms of wind and stability roses, before concentrating on CALPUFF results. Fig. 3 (A) reports the wind rose in the first vertical layer extrapolated from CALMET

Table 2
Point source characterization.

Point Source		
Stack height	9	[m]
Stack diameter	1.2	[m]
Odour emission rate (OER)	2000	[ou_E/s]
Exit temperature	313	[K]
Exit velocity	5.4	[m/s]

Fig. 1. Position of the site in Italy (left) and identification of the simulation domain (right).

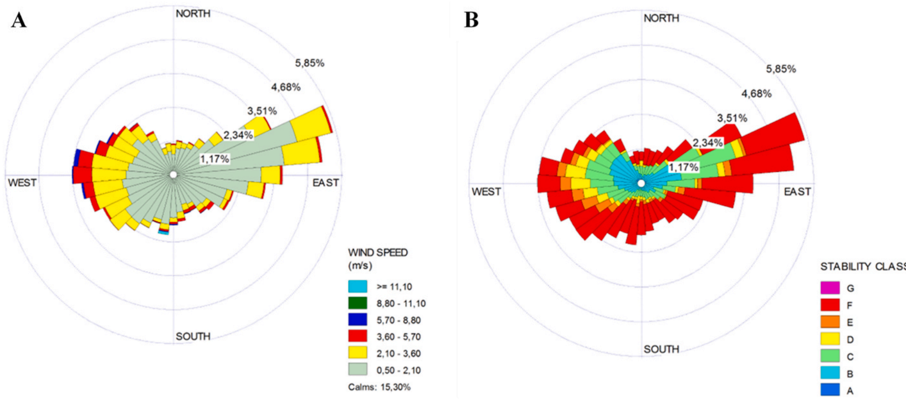

Fig. 3. Wind rose for the year 2016 for "METAR", "ERA5", "Relative Humidity" and "Solar Radiation" simulations (A). Stability rose for the year 2016 for "METAR" simulation (B).

simulations, indicating the main directions in which the wind blows. The graph shows that the prevailing winds are from east (E) and west (W) directions, with wind speeds that rarely exceed 10 m/s, with a calm percentage (i.e. wind speed <0.5 m/s) equal to 15.3%.

It is worth noting that the investigated different approaches to estimate CC data generate the same wind rose since CC has no effect on wind speed and wind direction and all the simulations process identical surface station data (except for CC).

The stability roses indicate the atmospheric stability class ranging from A (very unstable) to F/G (very stable) [17]. The stability classes were determined by the Pasquill-Gifford-Turner PGT scheme implemented in CALMET [28].

As an example, in Fig. 3 (B), the stability rose extrapolated from CALMET simulations run with METAR CC data is reported. The graph suggests that the atmosphere is predominantly stable, with a significant portion of neutral conditions. In order to avoid repetition of similar graphs, wind roses resulting from CALMET simulations with different CC data are not shown.

To investigate a possible effect of different CC choices, Fig. 4 shows frequencies (%) associated to PGT stability classes for each CALMET simulation. The plot shows that PGT stability classes are similar for all the approaches, with a prevalence of stable atmosphere present nearly 50% of the time.

The impact of CC on several micrometeorological measures, such as Monin-Obukov Length, Lmo, and Mixing Height, Hmix, is examined, in addition to the stability classes. Lmo is used to describe the effects of buoyancy on turbulent flows, notably in the lower tenth of the atmospheric boundary layer [17]. Lmo, in absolute value, is the altitude at which there is a balance between mechanical and thermal turbulence and therefore this value is in practice of the same order as the vertical extent of the surface layer. Convective situations are characterized by negative values of Lmo, while stable situations by a positive value. Mixing height (Hmix) is the extent or depth to which a pollutant, such as smoke or odour, may be dispersed by means of turbulence and diffusion [17].

Fig. 5 shows the variation of the abovementioned parameters as a result of different CC input data: it seems that all the calculation methods provide Lmo and Hmix largely overlapped. Lmo values indicate that the atmosphere is mostly stable, while the maximum Hmix level reaches 3000 m.

Therefore, from this preliminary analysis based on CALMET findings, it turns out that different choices of CC do not appear to have a remarkable impact on micrometeorological variables returned by CALPUFF meteorological processor.

3.2. *Odour impact maps*

Fig. 6 shows the obtained odour impact maps (zoomed in the simulation domain) resulting from the four different approaches to estimate CC: "METAR", "ERA5", "Relative Humidity" and "Solar Radiation".

To recall, the image refers to the 98th percentile of odour peak concentration values, on an annual basis. According to the available Italian guidelines in the field of odour [20], odour impact maps should include three reference odour concentration values (i.e. 1 ou_E/m^3, 3 ou_E/m^3, 5 ou_E/m^3), considering that.

- for 5 ou_E/m^3, 90–95% of the population perceives the odour;
- for 3 ou_E/m^3, 85% of the population perceives the odour;

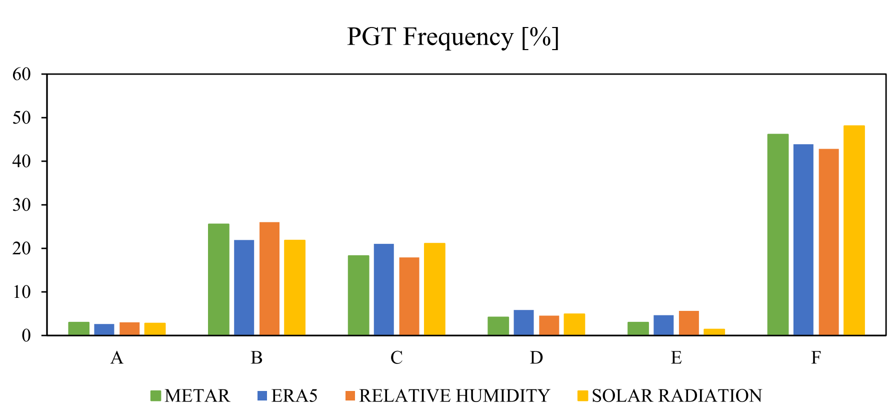

Fig. 4. Frequencies of the PGT stability classes for "METAR", "ERA5", "Relative Humidity" and "Solar Radiation" simulations.

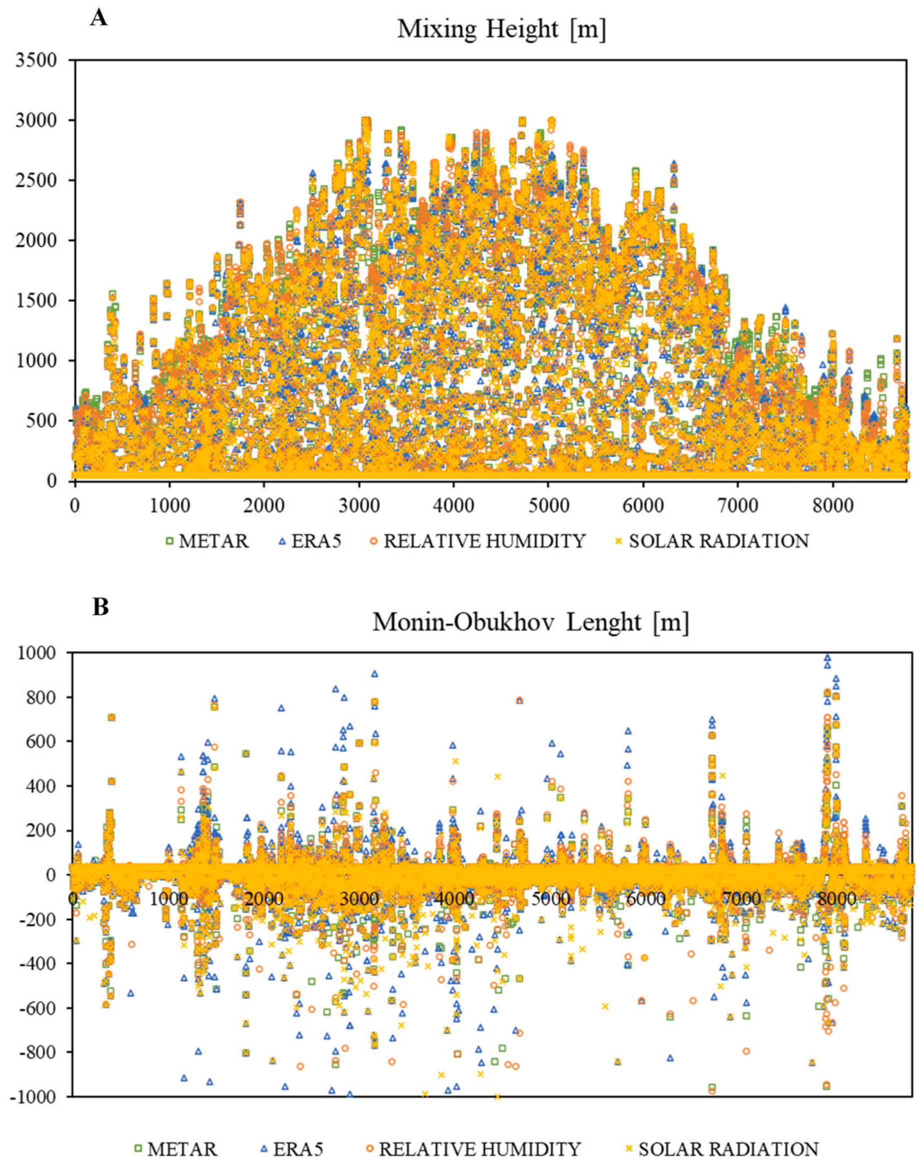

Fig. 5. Mixing Height (A) and Monin-Obukhov Lenght (B) for the year 2016 with METAR, ERA5, RELATIVE HUMIDITY and SOLAR RADIATION simulations.

- for 1 ou_E/m^3, 50% of the population perceives the odour.

As expected, for all simulations, the contour lines elongate more in the direction of the predominant winds, which are east (E) and west (W). By observing the contour maps, the most interesting outcome is that odour impact appears very similar, regardless of the chosen CC algorithm. Indeed, for all the simulations, the contour line referred to 5 ou_E/m^3 reaches a maximum distance of about 100 m, along the prevailing wind directions (E and W). For 3 ou_E/m^3, lines achieve a distance ranging from 100 m to 200 m. Then, considering the distance related to 1 ou_E/m^3, the maximum value is 400 m in the main wind directions (E and W).

3.3. Separation distances

Fig. 7 reports the direction-dependent separation distances, calculated according to Invernizzi et al. [40], for the three reference concentration values reported in the Italian guidelines (i.e. 1 ou_E/m^3, 3 ou_E/m^3, 5 ou_E/m^3), for all model runs: “ERA5”, “METAR”, “Relative Humidity” and “Solar Radiation”.

The separation distances associated to 5 ou_E/m^3 line (Fig. 7, A) appear almost overlapped for the four simulations. The same behaviour is observed for the other concentration levels (i.e. 3 ou_E/m^3 and 1 ou_E/m^3), with just a few irrelevant discrepancies.

The separation distance related to 5 ou_E/m^3 (Fig. 7, A) achieves a maximum value of roughly 100 m along the prevalent wind directions (E and W). Concerning the second reference concentration value (i.e. 3 ou_E/m^3) (Fig. 7, B), separation distances range from 100 m to 200 m. The greatest value in the main wind directions (E and W) is 400 m, associated to 1 ou_E/m^3 (Fig. 7, C).

In conclusion, as previously discussed for the odour contour maps, all the model runs (“ERA5”, “METAR”, “Relative Humidity” and “Solar Radiation”) simulated with different CC input data appear largely comparable.

4. Conclusions

In odour dispersion modelling, many sources of uncertainty should be taken into account, one of which is attributed to meteorological input data required by the model. As a result, it is crucial to identify the main sources of variability and to assess how this uncertainty will be reflected in the final results.

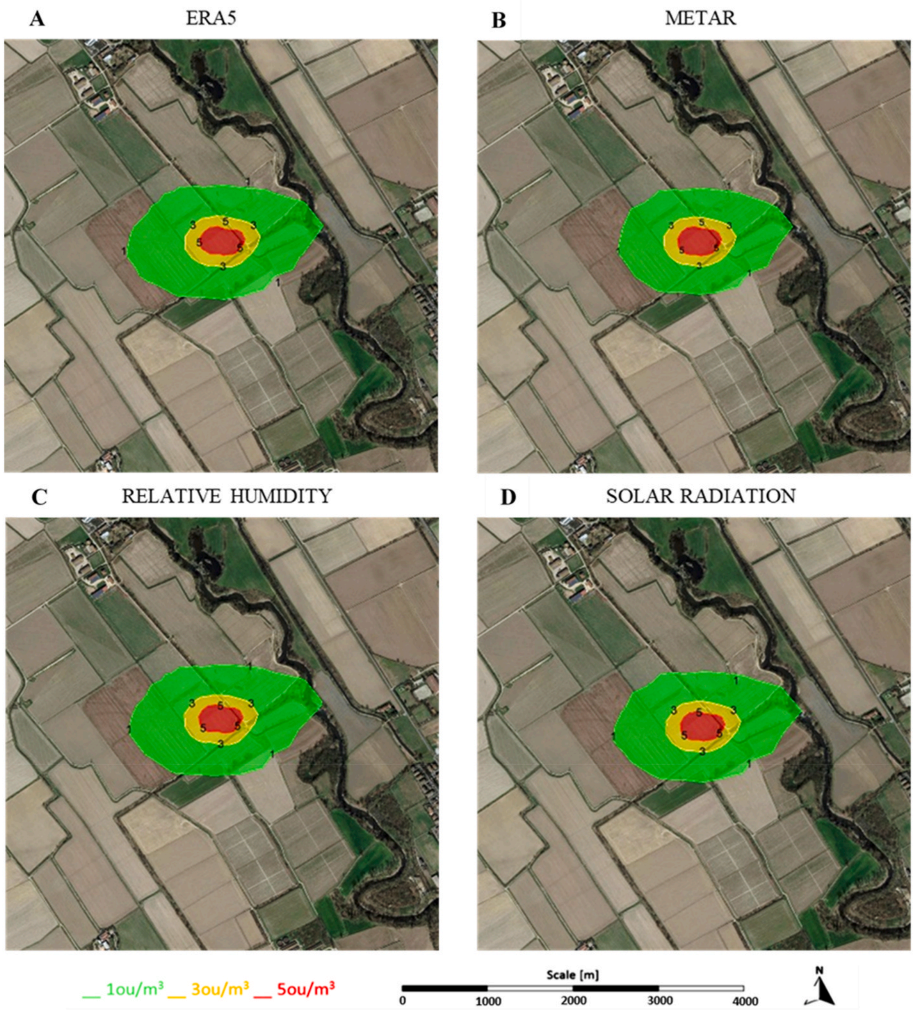

Fig. 6. Contour maps for the point source site for all model runs: "ERA5" (A), "METAR" (B), "Relative Humidity" (C) and "Solar Radiation" (D). The emission source is located in the centre of the odour impact maps.

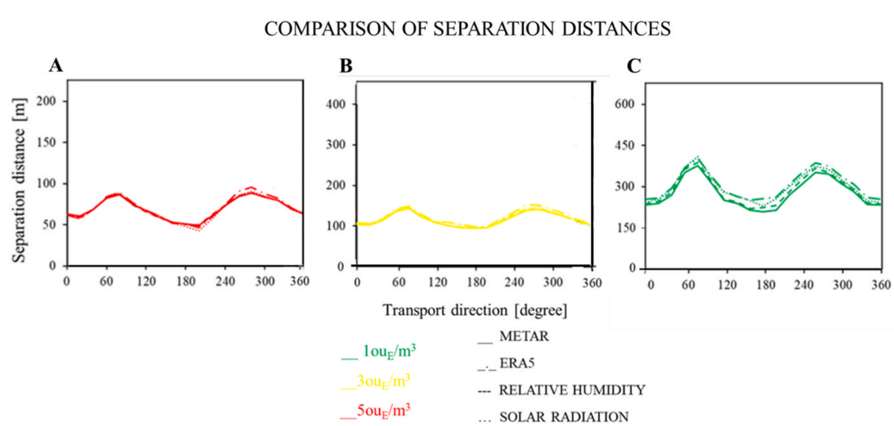

Fig. 7. Direction-dependent separation distances considering the point source site for all model runs: "ERA5", "METAR", "Relative Humidity" and "Solar Radiation". x-axis: direction (0° = north); y-axis: distance from the source. Red line (A) corresponds to 5 ou_E/m^3; yellow line (B) corresponds to 3 ou_E/m^3; green line (C) corresponds to 1 $ou_E/m.^3$. (For interpretation of the references to colour in this figure legend, the reader is referred to the Web version of this article.)

The current investigation provides information on how different numerical approaches to estimate CC values may affect CALPUFF outcome in odour impact assessment. This is a relevant finding, since CALPUFF is frequently adopted at the regulatory level.

The analysis considers a simulation domain located in the south of Milan, Italy, and it is based on odour impact criterion enforced in some Italian regions: the 98th percentile level of exceedance (on annual basis) is calculated for three concentration threshold levels (1 ou_E/m^3, 3 ou_E/m^3 and 5 ou_E/m^3).

From the model findings, all the simulations results appear to be largely comparable, as evidenced by CALMET output analysis of the micrometeorological parameters Monin-Obukhov length, Mixing Height, and PGT stability classes. Furthermore, simulated odour impact maps and separation distances appear almost overlapped. As a consequence, it can be inferred that CC calculation method, if properly applied, does not significantly influence odour impact assessment.

It should be pointed out that this research discusses a single case-study, so it focuses on a particular local condition, typical of the investigated simulation domain. Care should be taken in extrapolate the present result *as they are* in different orographic and meteorological situations.

As this work specifically focused on domains with flat orography, future investigation might be focused to evaluate the same analysis in a complex orography domain, since 3D reconstruction of wind fields is more challenging in a non-flat terrain. It would also be interesting to compare the results with the other MCLOUD options available in CALPUFF. These options suggest an internal calculation by CALMET to derive CC from the relative humidity values provided by the surface station, rather than processing CC data directly provided by the model user.

Finally, while this analysis is referred to a point source, it may be worthwhile to investigate whether the same results might be achieved using another type of source, such as an area source.

Declaration of competing interest

The authors declare that they have no known competing financial interests or personal relationships that could have appeared to influence the work reported in this paper.

Data availability

Data will be made available on request.

Supplementary Material

The supplementary material includes.

- Hourly surface meteorological observations provided by the Regional Agency for Environmental Protection (ARPA Lombardia, Milan, Italy) for the station of Landriano Cascina Marianna.
- Cloud cover data provided as CALMET input for the different investigated approaches.
- CALPUFF results (in terms of 98th percentile) on discrete receptors, for the different investigated approaches.

Appendix A. Supplementary data

Supplementary data to this article can be found online at https://doi.org/10.1016/j.cscee.2023.100492.

References

[1] S. Leogrande, et al., Industrial air pollution and mortality in the Taranto area, Southern Italy: a difference-in-differences approach, Environ. Int. 132 (2019), https://doi.org/10.1016/j.envint.2019.105030. Nov.
[2] J.E. Hayes, R.J. Stevenson, R.M. Stuetz, The impact of malodour on communities: a review of assessment techniques, Elsevier, Sci. Total Environ. 500–501 (2014) 395–407, https://doi.org/10.1016/j.scitotenv.2014.09.003. Dec. 01.
[3] M. Brancher, K.D. Griffiths, D. Franco, H. de Melo Lisboa, A review of odour impact criteria in selected countries around the world, Chemosphere 168 (2017) 1531–1570, https://doi.org/10.1016/j.chemosphere.2016.11.160. Elsevier Ltd.
[4] W. Dai, C. Otto, D. Reeves, Performing CALPUFF Analyses with Pseudo-station Data Derived from MM5 Data, 2000.
[5] A. Bokowa, et al., Summary and overview of the odour regulationsworldwide, Atmosphere 12 (2) (2021), https://doi.org/10.3390/atmos12020206. Feb.
[6] C. Bax, S. Sironi, L. Capelli, How can odors be measured? An overview of methods and their applications, Atmosphere 11 (1) (2020), https://doi.org/10.3390/atmos11010092. MDPI AG.
[7] M.T. Piccardo, M. Geretto, A. Pulliero, A. Izzotti, Odor emissions: a public health concern for health risk perception, Environ. Res. 204 (Mar. 2022), https://doi.org/10.1016/j.envres.2021.112121.
[8] M. Palmiotto, E. Fattore, V. Paiano, G. Celeste, A. Colombo, E. Davoli, Influence of a municipal solid waste landfill in the surrounding environment: toxicological risk and odor nuisance effects, Environ. Int. 68 (2014) 16–24, https://doi.org/10.1016/j.envint.2014.03.004.
[9] F. Tagliaferri, M. Invernizzi, S. Sironi, L. Capelli, Influence of modelling choices on the results of landfill odour dispersion, Detritus 12 (Sep. 2020) 92–99, https://doi.org/10.31025/2611-4135/2020.13998.
[10] H. Dourado, J.M. Santos, N.C. Reis, I. Mavroidis, Development of a fluctuating plume model for odour dispersion around buildings, Atmos. Environ. 89 (2014) 148–157, https://doi.org/10.1016/j.atmosenv.2014.02.053.
[11] K. de Hoogh, et al., Comparing land use regression and dispersion modelling to assess residential exposure to ambient air pollution for epidemiological studies, Environ. Int. 73 (Dec. 2014) 382–392, https://doi.org/10.1016/j.envint.2014.08.011.
[12] M. Piringer, W. Knauder, E. Petz, G. Schauberger, Factors influencing separation distances against odour annoyance calculated by Gaussian and Lagrangian dispersion models, Atmos. Environ. 140 (Sep. 2016) 69–83, https://doi.org/10.1016/j.atmosenv.2016.05.056.
[13] F. Tagliaferri, M. Invernizzi, L. Capelli, A sensitivity analysis applied to SPRAY and CALPUFF models when simulating dispersion from industrial fires, Atmos. Pollut. Res. 13 (1) (Jan. 2022), https://doi.org/10.1016/j.apr.2021.101249.
[14] H.A. Arregocés, R. Rojano, Sensitivity of the CALMET-CALPUFF model system on estimating PM10 concentrations at a mining site in northern Colombia, Case Studies in Chemical and Environmental Engineering 8 (Dec. 2023), 100402, https://doi.org/10.1016/j.cscee.2023.100402.
[15] R. Stull, Practical Meteorology an Algebra-Based Survey of Atmospheric Science, 2016. Vancouver, BC, Canada, http://www.eos.ubc.ca/books/Practical_Meteorology/. (Accessed 27 March 2023).
[16] World Meteorological Organization, Manual on the Observation of Clouds and Other Meteors, Secretariat of the World Meteorological Organization, 1975.
[17] R. Sozzi, et al., LA MICROMETEOROLOGIA E LA DISPERSIONE DEGLI INQUINANTI IN ARIA Agenzia per la Protezione dell'Ambiente e per i servizi Tecnici 2003, 2003 [Online]. Available: www.sinanet.apat.it.
[18] John S. Duncan, Aviation Weather Services, 2016 [Online]. Available: http://rgl.faa.gov/.
[19] F. Dogbey, P.J. Asilevi, J.F. Dzrobi, H.A. Koffi, N.A.B. Klutse, Modelling cloud cover climatology over tropical climates in Ghana, Atmosphere 13 (8) (2022), https://doi.org/10.3390/atmos13081265. Aug.
[20] Regione Lombardia. D.g.r. n. IX/3018 Determinazioni generali in merito alla caratterizzazione delle emissioni gassose in atmosfera derivanti da attività a forte impatto. odorigeno. 2012.
[21] Meteorological Monitoring Guidance for Regulatory Modeling Applications, 2000.
[22] Coordinamento Emissioni, Indirizzi per l'applicazione dell'articolo 272-bis del Dlgs 152/2006 in materia di emissioni odorigene di impianti e attività, 2023.
[23] J.S. Scire, D.G. Strimaitis, R.J. Yamartino, A User's Guide for the CALPUFF Dispersion Model, 2000.
[24] M. Rzeszutek, Parameterization and evaluation of the CALMET/CALPUFF model system in near-field and complex terrain - terrain data, grid resolution and terrain adjustment method, Sci. Total Environ. 689 (Nov. 2019) 31–46, https://doi.org/10.1016/j.scitotenv.2019.06.379.
[25] A.S. Rood, Performance evaluation of AERMOD, CALPUFF, and legacy air dispersion models using the Winter Validation Tracer Study dataset, Atmos. Environ. 89 (2014) 707–720, https://doi.org/10.1016/j.atmosenv.2014.02.054.
[26] H. Arregocés, R. Rojano, G. Restrepo, L. Angulo, Using CALPUFF to determine the environmental impact of a coal mine open pit, in: Air Pollution XXIV, WIT Press, 2016, pp. 55–66, https://doi.org/10.2495/air160061. Jun.
[27] Documentation of the Evaluation of CALPUFF and Other Long Range Transport Models Using Tracer Field Experiment Data, 2000.
[28] J.S. Scire, F.R. Robe, M.E. Fernau, R.J. Yamartino, A User's Guide for the CALMET Meteorological Model, 2000.
[29] J.L. The, R.F. Lee, The Effect of the CALMET Surface Layer Weighting Parameter R1 on the Accuracy of CALMET at Other Nearby Sites: a Case Study, 2003.
[30] A.L. Dresser, R.D. Huizer, CALPUFF and AERMOD model validation study in the near field: martins Creek revisited, J. Air Waste Manage. Assoc. 61 (6) (2011) 647–659, https://doi.org/10.3155/1047-3289.61.6.647.
[31] H. Hersbach, et al., The ERA5 global reanalysis, Q. J. R. Meteorol. Soc. 146 (730) (2020) 1999–2049, https://doi.org/10.1002/qj.3803. Jul.
[32] A. Van Delden, Atmospheric Dynamics, 2020 [Online]. Available: http://www.staff.science.uu.nl/delde102/AtmosphericDynamics.htm.
[33] C.J. Walcek, Cloud Cover and its Relationship to Relative Humidity during a Springtime Midlatitude Cyclone, AMS, 1994, https://doi.org/10.1175/1520-0493(1994)122<1021:CCAIRT>2.0.CO;2. Accessed: Apr. 06, 2023. [Online]. Available: .
[34] P.L. Llyn Escarcha, A.F. Pangue, B.P. Noreen Clemente, The Relationship between Cloud Cover to Temperature and Humidity, 2020.
[35] S.A. Kalogirou, Environmental Characteristics," in *Solar Energy Engineering*, Elsevier, 2014, pp. 51–123, https://doi.org/10.1016/b978-0-12-397270-5.00002-9.
[36] L. Luo, D. Hamilton, B. Han, Estimation of total cloud cover from solar radiation observations at Lake Rotorua, New Zealand, Sol. Energy 84 (3) (Mar. 2010) 501–506, https://doi.org/10.1016/j.solener.2010.01.012.
[37] A.A.M. Holtslag, A.P. Van Ulden, A Simple Scheme for Daytime Estimates of the Surface Fluxes from Routine Weather Data, 1983.

[38] F. Kasten, G. Czeplak, SOLAR AND TERRESTRIAL RADIATION DEPENDENT ON THE AMOUNT AND TYPE OF CLOUD, Pergamon Press Ltd, 1980.
[39] F. Dogbey, P.J. Asilevi, J.F. Dzrobi, H.A. Koffi, N.A.B. Klutse, Modelling cloud cover climatology over tropical climates in Ghana, Atmosphere 13 (8) (2022), https://doi.org/10.3390/atmos13081265. Aug.
[40] M. Invernizzi, M. Brancher, S. Sironi, L. Capelli, M. Piringer, G. Schauberger, Odour impact assessment by considering short-term ambient concentrations: a multi-model and two-site comparison, Environ. Int. 144 (2020), https://doi.org/10.1016/j.envint.2020.105990. Nov.